Food Chemistry: X 24 (2024) 101817

Contents lists available at ScienceDirect

Food Chemistry: X

journal homepage: www.sciencedirect.com/journal/food-chemistry-x

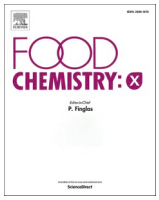

Investigating the effects of thermal processing on bitter substances in atemoya (*Annona cherimola* × *Annona squamosa*) through sensory-guided separation

Erh-Kang Luo [a], Chun-Ting Lin [a], Chao-Kai Chang [a], Nai-Wen Tsao [b], Chih-Yao Hou [c], Sheng-Yang Wang [b,d,e], Min-Hung Chen [f], Sheng-Yen Tsai [a], Chang-Wei Hsieh [a,g,h,i,*]

[a] *Department of Food Science and Biotechnology, National Chung Hsing University, South Dist., Taichung City 402, Taiwan*
[b] *Program in Specialty Crops and Metabolomics, Academy of Circle Economy, National Chung Hsing University, Nantou city 540, Taiwan*
[c] *Department of Seafood Science, National Kaohsiung University of Science and Technology, Nanzi Dist., Kaohsiung City 81157, Taiwan*
[d] *Department of Forestry, National Chung-Hsing University, Taichung City 402202, Taiwan*
[e] *Agricultural Biotechnology Research Center, Academia Sinica, Taipei City 115201, Taiwan*
[f] *Agriculture and Food Agency, Ministry of Agriculture, No.8 Guang-hwa Rd., Nantou county 540207, Taiwan*
[g] *Department of Food Science, National Ilan University, Shennong Road, Yilan City 26047, Taiwan*
[h] *Department of Medical Research, China Medical University Hospital, Taichung City 404333, Taiwan*
[i] *Advanced Plant and Food Crop Biotechnology Center, National Chung Hsing University, South Dist., Taichung City 402, Taiwan*

A R T I C L E I N F O

Keywords:
Atemoya
Bitterness
Untargeted identification
Liquid chromatography-high resolution mass spectrometry (LC-HRMS)
Orthogonal partial least-squares discrimination analysis (OPLS-DA)

A B S T R A C T

Atemoya (*Annona cherimola* × *Annona squamosa*) is a specialty crop in Taiwan. Thermal treatment induces bitterness, complicating seasonal production adjustments and surplus reduction. In this research, sensory-guided separation, metabolomics, and orthogonal partial least squares discrimination analysis (OPLS-DA) are used for identifying the bitterness in atemoya which originates from catechins, epicatechin trimers, and proanthocyanidins. Different thermal treatments (65 °C, 75 °C, and 85 °C) revealed that the glucose and fructose contents in atemoya significantly decreased, while total phenols, flavonoids, and tannins significantly increased. The concentration of 5-hydroxymethylfurfural (5-HMF) increased from 23.16 ng/g in untreated samples to 400.71 ng/g (AP-65), 1208.59 ng/g (AP-75), and 2838.51 ng/g (AP-85). However, these levels are below the 5-HMF bitterness threshold of 3780 ng/g. Combining mass spectrometry analysis with sensory evaluation, OPLS-DA revealed that atemoya treated at 65 °C, 75 °C, and 85 °C exhibited significant bitterness, with the main bitter components being proanthocyanidin dimers and trimers.

1. Introduction

Atemoya (*Annona cherimola* × *Annona squamosa*), a hybrid crop from the *Annona* genus in the *Annonaceae* family, is economically significant in Taiwan, with an export value of USD 51.8 million. (Wu et al., 2022). It is popular for its unique tropical flavor, nutrition, and various biological activities, including the hypolipidemic effect, anti-inflammatory activity, and antinociceptive effect (Moraes et al., 2021; Silva et al., 2017). Atemoya has a short post-harvest ripening period, leading to quality loss within 3 to 5 days (Ren et al., 2020). Studies have developed few postharvest treatments for prolonging the shelf-life. It was extended the storage period of atemoya from 18 to 30 days under low temperature through pulse electric field pretreatment (Chang et al., 2023). However, to achieve a significant extension of the storage period and promote commercial value, processing technologies to develop products of atemoya are necessary. Thermal processing and dehydration are common methods to extend fruit preservation. However related research pointed out that whether commercially sterilized puree or freeze-dried atemoya, had an unacceptable bitter taste (Baskaran et al., 2016). This bitterness is not well-documented due to the fruit's traditional consumption in its fresh form.

Atemoya is rich in carbohydrates and phytochemicals (de Moraes

* Corresponding author at: Department of Food Science and Biotechnology, National Chung Hsing University, South Dist., Taichung City 402, Taiwan
E-mail addresses: g110043108@mail.nchu.edu.tw (E.-K. Luo), chuntinglin@nchu.edu.tw (C.-T. Lin), kai70219@nchu.edu.tw (C.-K. Chang), nwt1228@dragon.nchu.edu.tw (N.-W. Tsao), taiwanfir@dragon.nchu.edu.tw (S.-Y. Wang), cmh@mail.afa.gov.tw (M.-H. Chen), 7111043211@smail.nchu.edu.tw (S.-Y. Tsai), welson@nchu.edu.tw (C.-W. Hsieh).

https://doi.org/10.1016/j.fochx.2024.101817
Received 28 May 2024; Received in revised form 4 September 2024; Accepted 4 September 2024
Available online 11 September 2024

et al., 2021). The sucrose in the pulp is converted into glucose and fructose, leading to the occurrence of both Maillard and caramelization reactions. Through the Maillard reaction pathway, glucose and fructose react with proteins and amino acids via an amine-carbonyl reaction to form Schiff bases. In an acidic environment (pH $\leq$ 7), 3-deoxyglucosone (3-DG) is produced following 1,2-enolization, dehydration, and deamination. A series of dehydration steps then results in the formation of the bitter Maillard reaction product 5-hydroxymethylfurfural (5-HMF) and subsequent compounds (Capuano & Fogliano, 2011; Gökmen et al., 2007). Similarly, 3-DG may also be formed from the 1,2-enolization and dehydration of glucose and fructose via the caramelization pathway, leading to the production of bitter substances such as 5-HMF, 5-methylfurfural (5-MF), and subsequent reaction products (Li et al., 2021; Niwa, 1999). However, the release of phytochemicals due to thermal processing, followed by subsequent degradation and polymerization, is also one of the reasons for developing bitterness (Degenhardt & Hofmann, 2010). High temperatures processing and the acidic conditions of atemoya pulp induce decomposition, polymerization, and oxidation reactions, releasing phytochemicals from cell vacuoles and increasing soluble phytochemicals (Feumba Dibanda et al., 2020; Shiratake & Martinoia, 2007), and lead to phytochemical binding to cell wall structural components such as cellulose, hemicellulose, and pectin. The release of phytochemicals leads to an increase in soluble phytochemicals (Acosta-Estrada et al., 2014; Liu et al., 2017), resulting in a bitter taste. Li et al. (2020) mentioned that heating can also cause phytochemicals to condense with carbohydrates, proteins, pectins, and other substances into insoluble phenolics. Therefore, the impact of thermal processing on the phytochemical content varies depending on the composition and types of phytochemicals present in the fruit. However, the specific compounds responsible for the development of bitterness in atemoya pulp during thermal processing remain to be clarified.

Although the study of bitter compounds and their transformations during heat treatment has been extensively conducted in many crops, such as tea and coffee, similar investigations are lacking for atemoya. Metabolomics is a scientific method employed to identify low molecular weight metabolites within the metabolic pathways of organisms. According to BitterDB (http://bitterdb.agri.huji.ac.il/dbbitter.php), most molecules have a molecular weight of less than 1000. Utilizing this characteristic, sesomics will be applied to identify the bitter substances present in atemoya (Yang et al., 2021). Sensory-guided fractionation, widely used to effectively identify bitter compounds, combines chromatography and sensory evaluation (Pu et al., 2017; Yang et al., 2021). Furthermore, orthogonal partial least-squares discrimination analysis (OPLS-DA) can be used to identify compounds that significantly differ among species (Gao et al., 2019; Yang et al., 2022), while orthogonal partial least-squares (OPLS) analysis can pinpoint compounds that primarily contribute to bitter intensity (Gao et al., 2021, 2023). Therefore, utilizing the analysis of differences between species in tandem with OPLS-DA, combined with sensory-guided fractionation and OPLS, can effectively screen for bitterness.

Soursop (*Annona muricata*) is one of the *Annona* species that does not develop bitterness upon heating, making it suitable for various processed products (Baskaran et al., 2016). In this research, soursop and atemoya were selected for OPLS-DA, sensory-guided fractionation, and OPLS analysis. The results, which identified the key molecules contributing to bitterness in atemoya after heat processing, provide a foundation for potential methods to reduce the bitterness in atemoya products.

2. Materials and methods

2.1. Sample preparation

Atemoya (*Annona cherimola* × *Annona squamosa*), weighing 450 ± 50 g at commercial ripeness, were acquired from Beinan Township, Taitung County, Taiwan, in February 2023. Soursop, weighing 1800 ± 100 g at 90 % ripeness, was acquired from Zhutian Township, Pingtung County, Taiwan, during the same period. Only fruits without visible diseases or physical damage were selected for the study. After removing the peels and seeds, the pulp was homogenized using a blender (12-speed Osterizer blender Oster, Oster®, USA) and freeze-dried (YFD-100, Yu Shing Bio-Tech Co., Ltd., Taiwan) to obtain untreated samples. This approach was undertaken to explore the native bitter compounds in atemoyas.

For thermal treatment, the atemoya was homogenized, sealed, and subjected to heat treatment at 65 °C, 75 °C, and 85 °C for 30 min (Baskaran et al., 2016), resulting in samples labeled AP-65, AP-75, and AP-85 respectively. These samples were then freeze-dried. Both the untreated and thermal treatment samples were subjected to subsequent mass spectrophotometry analysis to determine their components and investigate the causes of bitterness in atemoyas after thermal treatment.

2.2. Total phytochemical content of samples

One gram of sample was extracted with 20 mL of 80 % ethanol (Katayama Pure Chemical Co., LTD., Changhua County, Taiwan) subjected to ultrasound-assisted extraction (28 kHz, 400 W; TST-TP, Taiwan Supercritical Technology Co., Ltd., Taichung City, Taiwan) for 15 min, the temperature remains stable at 25 °C by closely monitoring it with a thermometer (TES-1306, TES Electrical Electronic Crop., Taipei, Taiwan). The mixture was then centrifuged at 12,000 ×*g* for 20 min, and the supernatant was collected for subsequent testing. (Wei et al., 2021).

2.2.1. TPC

25 μL of extract was added to 125 μL of Folin–Ciocalteu's phenol reagent (PanReac AppliChem, Spain) in a microcentrifuge tube and reacted for 3 min. Then, 100 μL of sodium carbonate (99 %, Katayama Chemical Co., Ltd., Japan) solution (7.5 %, m/v) was added and incubated in the dark for 1 h. The absorbance was measured at 760 nm (Spectrophotometer 1510-02050, Thermo Fisher Scientific, MA, USA). Gallic acid (99.5 %, Scharlau, Barcelona, Spain) was used for standard calibration, ranging from 0 to 200 μg mL^{-1} (Moraes et al., 2021).

2.2.2. Total flavonoid content (TFC)

100 μL of the extract was mixed with 300 μL of 95 % ethanol, 20 μL of 10 % aluminum chloride (97 %, Katayama Chemical Co., Ltd., Osaka, Japane), and 20 μL of 1 M potassium acetate (Sigma-Aldrich, MA, USA) in a microcentrifuge tube and then kept for 30 min. The absorbance was measured at 415 nm (Spectrophotometer 1510-02050, Thermo Fisher Scientific, MA, USA), and quercetin (95 %, Acros Organics, NJ, USA) was used for standard calibration, ranging from 0 to 200 μg mL^{-1} for comparison (Ng & Tan, 2017).

2.2.3. Total tannin content (TTC)

A gram of atemoya sample was combined with 80 % ethanol, and the resulting mixture was subjected to homogenization followed by ultrasonic treatment for 15 min. Subsequently, the solution underwent centrifugation at 12,000*g* for 15 min, after which the supernatant was collected. This procedure was repeated thrice, and the collected supernatants were amalgamated to form the tannin phenolic extract. To the extract, 100 mg of polyvinylpolypyrrolidone (PVPP; AK Scientific, Union City, USA) was added along with 1.0 mL of deionized water, and the mixture was agitated for 15 min. Post-centrifugation at 12,000*g* for 15 min (CT18R, Himac, Tokyo, Japan), the supernatant was collected as the non-tannin phenolic fraction.

For each treatment, two types of solutions were prepared before and after PVPP treatment. The absorbance at 725 nm was measured for both solutions, and tannic acid (Daejung, Siheung-si, Korea) was used for standard calibration, ranging from 0 to 200 μg mL^{-1} (Kalalinia et al., 2020). The formula was calculated as follows (1):

$$\text{Tannins}\ (\%) = \text{Total phenolics}\ (\%) - \text{non tannin phenolics}\ (\%) \quad (1)$$

2.3. Fructose, glucose and sucrose

Sample 200 mg was mixed with 10 mL of deionized water, and then 1 mL of this mixture was filtered into a vial bottle using a syringe through a 0.22 μm filter membrane (Syringe filter PVDF-L 0.22 μm, Waters, MA, USA). The Hitachi HPLC system, equipped with a high-performance liquid chromatography pump (Chromaster 5110, Hitachi, Japan) and an automatic sampler (Chromaster 5260, Hitachi, Tokyo, Japan) was utilized for the analysis. The oven temperature was maintained at 25 °C, and the sample injection volume was set to 20 μL. Chromatography separation was performed using Luna NH2 column (250 × 4.6 mm, 5 μm, Phenomenex, CA, USA). Fructose, glucose, and sucrose were separated using equal gradient elution with a mobile phase of 75 % acetonitrile aqueous solution (> 99.9 %, Honeywell International Inc., NC, USA). The elution was performed at a surface flow rate of 1 mL/min with a refractive index detector (Chromaster 5450, Hitachi, Tokyo, Japan) (Singh & Vij, 2018).

2.4. 5-Hydroxymethylfurfural (5-HMF)

Sample powder 2 g was added to 20 mL of 80 % methanol, stirred thoroughly, and extracted in three batches at 25 °C using an ultrasonic water bath for 15 min. The supernatant was filtered through a 0.22 μm filter membrane (Syringe filter PVDF-L 0.22 μm, Waters, MA, USA) using a syringe and 1 mL of sample/standard was transfered into a vial bottle. The analysis was conducted using a Hitachi HPLC system equipped with a high-performance liquid chromatography pump (Chromaster 5110, Hitachi, Japan) and an automatic sampler (Chromaster 5260, Hitachi, Tokyo, Japan). The oven temperature was set to 25 °C, with a sample injection volume of 20 μL. The separation was performed on a Mightysil RP-18 GP column (4.6 × 250 mm, 5 μm, Kanto Chemical, Tokyo, Japan) (Singh & Vij, 2018). The mobile phase was washed with an equal gradient of deionized water: acetonitrile (88:12, *v*/v) for 10 min at a flow rate of 1.0 mL/min and detected at a wavelength of 284 nm (UV-VIS Detector 5420, Hitachi, Tokyo, Japan).

2.5. Degree of proanthocyanin

In the mass analysis of proanthocyanidins, 1.0 mL of sample was mixed with 3.0 mL vanillin-methanol reagent (40 mg/mL) and 1.5 mL concentrated hydrochloric acid. The mixture was sealed in a tube, vigorously shaken for 10 s, and allowed to react at 25 ± 1 °C for 15 min. The absorbance of the solution was measured at 500 nm. Cathecin was weighed 2 mg, dissolved in methanol to a final volume of 10 mL, and used to prepare a standard curve ranging from 0 to 200 μg mL^{-1}.

For proanthocyanidins content analysis, the sample was re-dissolved in 1 mL of methanol and brought up to 25 mL with acetic acid. A volume of 1.0 mL of the diluted sample or standard solution was combined with 5.0 mL of reaction reagent (1 % vanillin (*w*/*v*), 4 % HCl (*v*/v) acetic acid reagent). The reaction was carried out at 25 ± 1 °C for 15 min. The absorbance of the solution was then measured at 500 nm using a UV spectrophotometer. Additionally, 5.0 mg of catechin was dissolved in 1 mL of methanol, and the volume was adjusted to 25 mL with acetic acid to prepare a standard curve (Chen et al., 2016). The average degree of proanthocyanin was subsequently calculated as:

$$\text{mDP (mean degree of polymerization)} = \frac{m}{\text{Mn}} \quad (2)$$

m: average mass of proanthocyanidins (μg)
n: Substance content of proanthocyanidins (μmol)
M: Molecular weight of monomeric catechin

2.6. High-Resolution Liquid Chromatography Mass Spectrometer (LC-HRMS) analysis

The extracts were prepared in a 30 mg/mL methanol solution and filtered through a PVDF-L syringe filter with a 0.22 μm pore size membrane. Analysis was conducted using LC (LC-20 CE XR, Shimadzu, Tokyo, Japan) coupled with an HRMS (Orbitrap Exploris™ 120, Thermo Fisher Scientific, MA, USA) employing electrospray ionization. Chromatographic separation was carried out with the PuriFlash 100 A C18 XS column (250 × 4.6 mm, 5 μm). The mobile phase consisted of (A) 5 mM ammonium acetate (Sigma-Aldrich, MA, USA) and (B) acetonitrile for the positive mode and (A) 0.5 % formic acid and (B) acetonitrile for the negative mode. The flow rate was set to 0.6 mL/min, with an injection volume of 20 μL. The mobile phase gradient is 0–1 min, 2 % solvent B; 1–14 min, 2 %–15 % solvent B; 14–19 min, 15 %–20 % solvent B; 19–19.5 min, 20 %–95 % solvent B; 19.5–21 min, 95 % solvent B; 21–21.5 min, 95 %–2 % solvent B; 21.5–28 min, 2 % solvent B. The mass spectrometry parameters were set. The mass spectrometry scan range was set from 100 to 1000 *m/z*. The temperatures of both the ion transfer tube and vaporizer were 350 °C. Spray voltages were adjusted to 3.5 kV for the positive mode and 2.5 kV for the negative mode. The sheath gas, auxiliary gas, and sweep gas were set at 60, 15, and 2 arb, respectively. The alignment, deconvolution, ion extraction, and integration of full-scan MS data were conducted with an acquisition software (Xcalibur 4.0.27; Thermo Fisher Scientific, MA, USA), combined with PubChem (https://pubchem.ncbi.nlm.nih.gov/), ChemSpider (http://www.chemspider.com/), mzCloud (https://beta.mzcloud.org/), MassBank (https://massbank.eu/MassBank/), and NIST MS Search 2.0 databases for peak annotation (https://chemdata.nist.gov/).

2.7. Sensory-guided fractionation

Bitter compounds in plant tissues can be extracted using ethanol because of their low polarity and hydrophobic characteristics (Pu et al., 2017). The pulp powder was extracted with 95 % ethanol (Katayama Pure Chemical Co., Ltd., Osaka, Japan) at a solid-liquid ratio of 1:20 (*w*/*v*), accompanied by 28 kHz, 400 W ultrasonic extraction at 25 °C for 20 min. The ethanol fraction of the extract was removed by rotary evaporation (R-2000S, Panchum Scientific Corp., Kaohsiung City, Taiwan) at 45 °C water bath (B1, Panchum Scientific Corp., Kaohsiung City, Taiwan) and subsequently freeze-dried. The extract of the ethanol fraction was labeled F-I, whereas the residue of the insoluble fraction was labeled F-II.

The F-I powder was dissolved in 5 mL of 95 % ethanol and diluted to 100 mL of deionized water (Arium® Pro Ultrapure Water Systems, Göttingen, Germany). The F—I solution was extracted with *n*-hexane (3 × 100 mL) (95 %, Daejung, Siheung-si, Korean), and the upper phase was collected as the *n*-hexane fraction (F-I-A). The lower phase solvent was evaporated using rotary evaporation at 45 °C and dispersed in deionized water with a small amount of ethanol. This extraction process was repeated to obtain the ethyl acetate (≥99.5 %, Honeywell, Charlotte, NC, USA) fraction (F-I-B), the *n*-butanol (ECHO Chemical Co., Ltd., Miaoli County, Taiwan) fraction (F-I-C) subsequently, and the remaining aqueous layer extracts (F-I-D). After the solvent was completely removed from each fraction, the samples were freeze-dried to yield the respective powdered fractions (Pu et al., 2017).

2.8. Sensory analysis

A reference solution of caffeine (Sigma-Aldrich, MA, USA) was employed to evaluate bitterness intensity. Panelists were offered three samples in the tasting session; distilled water and two caffeine solutions (*w*/w) with concentrations varying between 0.03 % and 0.15 %. These concentrations were designed to align with a bitterness intensity scale ranging from 2 to 10. This approach aims to establish the panelist's ability to discern bitterness level accurately, establishing a reliable

baseline for bitterness perception (Bin & Peterson, 2016).

Ten panelists (5 women and 5 men) aged 22–30 years without oral-related diseases were selected for subsequent sensory evaluation tests. The sensory evaluation was based on a 10-point scale, with 1 being the least and 10 being the most bitter (Civille & Carr, 2015; Pu et al., 2017; Yang et al., 2021). The sensory evaluation in this study was approved by the National Cheng Kung University Medical College-Human Research Ethics Review Committee (Application code B-ER-111-438). All participants were informed about the study and provided written informed consent to participate in the study.

2.9. Statistical and multivariate analyses

Data analysis was conducted with IBM SPSS Statistics version 20.0 (IBM Corp, Armonk, NY, USA). A two-tailed unpaired *t*-test was used to analyze statistical differences between two species, the one-way analysis of variance was used for statistical comparisons among multiple groups, and Duncan's multiple-range test was used for post hoc testing. A *p*-value of <0.05 was determined as statistically significant. SIMCA (14.1, Umetrics, Umea, Sweden) was used for the multivariate analysis of the LC-HRMS chemical profile. The peak area of the chemical profile was normalized with Pareto scaling, and then the principal component analysis (PCA), orthogonal projections to the OPLS-DA, and OPLS were established (Qin et al., 2020). In the OPLS model, the peak area and bitterness intensities of the compounds were set as X and Y variables, respectively. The quality levels of OPLS-DA and OPLS models were evaluated by R^2X, R^2Y, and Q^2 values, where R^2X and R^2Y represent the explanatory rates of matrices X and Y, respectively, indicating the accuracy of the fit, whereas Q^2 represents the predictive ability of the model. Both OPLS-DA and OPLS models were validated by permutation analysis (200 times). Variable importance parameter (VIP) scores were calculated to evaluate the contribution of the model and compounds with VIP values >1 were considered significantly different compounds. The heatmaps of the compounds were generated using GraphPad Prism 8.0 (GraphPad, Boston, MA, USA) (Gao et al., 2023; Wei et al., 2021).

3. Results and discussion

3.1. Phytochemical content in soursop and atemoya

Atemoya is rich in phenolic acids, flavonoids, and their derivatives. However, these phytochemicals often contribute to the bitter taste of the fruit. Therefore, quantification was necessary to determine whether a higher concentration of phytochemicals is responsible for the increased bitterness in atemoya compared to soursop. In Table 1, the result show that the bitterness intensity of freeze-dried atemoya significantly increased, whereas freeze-dried soursop did not exhibit the same effect. Since freeze-drying removes water without triggering additional chemical reactions (Elmas et al., 2019), we hypothesized that the unprocessed atemoya flesh likely contains substantial levels of bitter compounds or their precursors.

The TPC, TFC, and TTC in atemoya were 3.76 ± 0.20 mg/g, 0.40 ± 0.01 mg/g, and 2.74 ± 0.13 mg/g, respectively, and 3.60 ± 0.14 mg/g, 1.64 ± 0.09 mg/g, and 1.40 ± 0.12 mg/g in soursop, respectively (Table 1). The total phenolic content (TPC) results showed no significant difference between the two species. Although the total flavonoid content in soursop is four times higher than.

that in atemoya, the expression of bitterness requires compounds with specific structures that are capable of binding to human bitter taste receptors (Xiang et al., 2024). Relevant literature indicates that the expression of bitter taste is not necessarily positively correlated with concentration but is rather a threshold value. Furthermore, the functional groups and configuration of phytochemicals also affect taste (Chen et al., 2022b). Therefore, while this part of the research can only speculate, it is evident that although soursop and atemoya belong to the same genus, their phytochemical contents are significantly different, which may result in different effects on flavor presentation.

3.2. Potential bitter compounds in atemoya

Thirty-three compounds were identified as potential bitter compounds, including 17 phenolic acids and their derivatives, 11 flavonoids and their derivatives, 4 proanthocyanidins, and 1 cyclohexylcarboxylic acid (Table 2.). The PCA biplot was generated by importing the peak area of the potential bitter compounds in atemoya and soursop. It was used to exhibit the variation of the potential bitter compounds between two *Annona* species (Fig. 1a). The sum of the principal components explained 99.5 % of the total variance, which was considered acceptable as reached 70 %–80 % (Suhr, 2005). In the PCA plot, the variables A1–A3 and S1–S3 represent the variable points for the atemoya and soursop sample groups, respectively, while C1–C33 represent the variable points for potential bitter compounds, with the numerical sequence corresponding to the first column in Table 2. The distance between the sample group variables and the potential bitter compound variables in the principal component coordinate plot indicates their correlation; the closer the distance, the stronger the correlation between the two. The results revealed that the variables of atemoya and soursop were distributed over the first principle component axes, indicating a significant difference in the composition of potential bitter substances between the two species. Afterward, the variable of atemoya was closely related to the variable of bitter intensity, which is caused by a stronger bitter intensity in atemoya. Thus, the 22 variables of the bitter compounds close to the variables of atemoya highly correlated with bitter intensity, including catechin, protocatechuic acid, quercetin-3-*O*-glucoside, vanillic acid, sinapic acid, two isomers of procyanidin trimer, two isomers of procyanidin dimer, quinic acid, ferulic acid, epicatechin, cinnamic acid, 4-(*β*-D-glucopyranosyloxy)benzoic acid, caffeic acid-3-*O*-glucuronide, gallic acid-4-*O*-glucoside, hydroxybenzoic acid hexoside, *p*-coumaric acid, *p*-coumaric acid methyl ester, salicylic acid, 2-methoxy-5-prop-1-enylphenol, and isopeonidin 3-*O*-arabinoside. Most

Table 1
Bitter intensity, total phenolics, total flavonoids, and total tannins content of the freeze-dried pulp and the fresh pulp of *A. cherimola* × *A. squamosa* and *A. muricata*.

Sample	Treatment	Water content (%)	Bitterness	Total phenolics content (mg/g DW)	Total flavonoids content (mg/g DW)	Total tannins content (mg/g DW)
A. cherimola × *A. squamosa*	Fresh	72.41	1.21 ± 0.25^{b}	–	–	–
	Freeze-dried	14.46	6.30 ± 1.09^{a}	3.76 ± 0.01^{b}	0.40 ± 0.01^{b}	2.74 ± 0.13^{a}
A. muricata	Fresh	85.22	1.25 ± 0.25^{b}	–	–	–
	Freeze-dried	13.92	1.38 ± 0.56^{b}	3.60 ± 0.14^{a}	1.64 ± 0.09^{a}	1.40 ± 0.17^{b}

The average of bitter intensities was valued by 10 panelists ($n = 10$, male/female = 1:1). $^{a\text{-}b}$ mean the data were significantly different in the same column ($p < 0.05$).
Fresh: Unheated pulp
Freeze-dried: Unheated and dehydrated pulp

Table 2
Bitter compound analysis of *A. cherimola* × *A. squamosa* and *A. muricate* with different thermal treatments (Fresh Atemoya, Fresh Soursop, AP-65, AP-75 and AP-85).

Compound No.	Tentative assignment	RT (mins)	m/z exp	m/z calc	Ion mode	Molecular formula	Peak area					Bitter threshold	Reference
							Fresh Atemoya	Fresh Soursop	(AP-65)	(AP-75)	(AP-85)		
1	Catechin	3.3	289.0713	289.0718	NEG	$C_{15}H_{14}O_6$	16,703,801	2,148,815	33,291,565	21,084,173	22,040,813	1000 μM	Hufnagel and Hofmann (2008)
2	Protocatechuic acid	3.54	153.0191	153.0193	NEG	$C_7H_6O_4$	2,464,589	113,050	2,733,145	2,699,142	2,543,843	155.64 μM (TAS2R14)	Soares et al. (2018)
3	Quercetin-3-O-glucoside	5.81	463.0881	463.0882	NEG	$C_{21}H_{20}O_{12}$	2845	1211	3321	4489	5898	28 μM	Dresel et al. (2015)
4	Vanillic acid	5.53	169.0495	169.0495	POS	$C_8H_8O_4$	13,088,923	29,178	18,713,270	17,459,303	13,846,317	315 μM	Hufnagel and Hofmann (2008)
5	Sinapinic acid	3.59	223.0611	223.0612	NEG	$C_{11}H_{12}O_5$	14,414,597	5,412,002	13,399,211	11,332,901	10,044,889	4.46 μM	Rubino et al. (1996)
6	Procyanidin trimer isomer 1	14.51	865.1955	865.1985	NEG	$C_{45}H_{38}O_{18}$	2,331,109	65,779	3,974,101	4,076,632	8,549,796	400 μM	Hufnagel and Hofmann (2008)
7	Procyanidin trimer isomer 2	16.42	865.1987	865.1985	NEG	$C_{45}H_{38}O_{18}$	13,065,728	32,707	84,137,513	105,049,191	70,018,055	400 μM	Hufnagel and Hofmann (2008)
8	Procyanidin dimer isomer 1	3.42	577.1379	577.1375	NEG	$C_{30}H_{26}O_{12}$	6,250,063	12,658	52,141,744	62,134,566	90,187,451	500 μM	Hufnagel and Hofmann (2008)
9	Procyanidin dimer isomer 2	3.77	577.1379	577.1375	NEG	$C_{30}H_{26}O_{12}$	32,618,833	503,539	170,645,921	190,730,946	1.55E+08	500 μM	Hufnagel and Hofmann (2008)
10	Quinic acid	8.09	191.0560	191.0561	NEG	$C_7H_{12}O_6$	4,024,794	872,957	4,165,573	5,338,476	10,275,044	52 μM	Frank et al. (2006a)
11	Ferulic acid	3.54	193.0505	193.0505	NEG	$C_{10}H_{10}O_4$	8,872,462	4,369,312	8,422,314	7,536,315	6,470,552	710 μM	Soares et al. (2018)
12	Epicatechin	3.41	289.0715	289.0717	NEG	$C_{15}H_{14}O_6$	50,923,829	1,726,606	43,892,029	30,489,800	21,608,567	860 μM	Chen et al. (2022a)
13	Cinnamic acid	13.2	147.0450	147.0451	NEG	$C_9H_8O_2$	446,164	113,070	521,187	647,260	733,321	938 μM	Habschied et al. (2021)
14	4-(β-D-glucopyranosyloxy) benzoic acid	17.19	299.0768	299.0767	NEG	$C_{13}H_{16}O_8$	3,028,127	606,200	3,177,643	3,292,134	3,440,893	–	Banerjee and Preissner (2018a)
15	Caffeic acid 3-O-glucuronide	4.11	355.0670	355.0670	NEG	$C_{15}H_{16}O_{10}$	35,839	308	30,221	21,335	15,150	–	Banerjee and Preissner (2018a)
16	Gallic acid 4-O-glucoside	8.84	331.0669	331.0670	NEG	$C_{13}H_{16}O_{10}$	2,426,145	294,141	130,810	69,931	17,628	–	Banerjee and Preissner (2018a)
17	Hydroxybenzoic acid hexoside	17.19	299.0757	299.0754	NEG	$C_{13}H_{16}O_8$	3,042,900	28,304	2,411,789	1,844,521	1,500,083	–	Banerjee and Preissner (2018a)
18	p-Coumaric acid	3.57	165.0546	165.0546	POS	$C_9H_8O_3$	9,092,883	6,569,415	11,209,486	13,511,662	12,510,639	290 μM	CHuang and Zayas (1991)
19	p-Coumaric acid methyl ester	5.54	179.0701	179.0703	POS	$C_{10}H_{10}O_3$	2,239,293	975,832	2,325,314	2,923,441	2,436,607	189 μM	Dresel et al. (2015)
20	Salicylic acid	5.56	139.0393	139.0390	POS	$C_7H_6O_3$	8,178,451	6,172,212	7,996,863	7,907,499	7,841,070	–	Banerjee and Preissner (2018a)
21	2-Methoxy-5-prop-1-enylphenol	6.5	165.0908	165.0910	POS	$C_{10}H_{12}O_2$	24,524	11,235	21,445	17,831	15,179	–	Banerjee and Preissner (2018a)
22	Isopeonidin 3-O-arabinoside	16.4	434.1220	434.1209	POS	$C_{21}H_{21}O_{10}$	2,528,633	477,954	2,548,841	2,655,431	2,750,406	–	Banerjee and Preissner (2018a)

(*continued on next page*)

Table 2 (*continued*)

Compound No.	Tentative assignment	RT (mins)	m/z exp	m/z calc	Ion mode	Molecular formula	Peak area					Bitter threshold	Reference
							Fresh Atemoya	Fresh Soursop	(AP-65)	(AP-75)	(AP-85)		
23	3-Caffeoylquinic acid	10.06	353.0877	353.0878	NEG	$C_{16}H_{18}O_9$	4008	916,597	7210	4210	1180	1019 μM	Sun et al. (2023)
24	Rosmarinic acid	8.95	359.0777	359.0772	NEG	$C_{18}H_{16}O_8$	411	10,728	476	313	188.0000	102 μM	García et al. (2016)
25	Rutin isomer 1	13.59	609.1467	609.1461	NEG	$C_{27}H_{30}O_{16}$	5500	32,109	2040	921	320	117 μM	Chen et al. (2023)
26	Rutin isomer 2	13.98	609.1464	609.1461	NEG	$C_{27}H_{30}O_{16}$	3872	19,592	4151	3520	3250	117 μM	Chen et al. (2023)
27	Rutin isomer 3	14.31	609.1450	609.1461	NEG	$C_{27}H_{30}O_{16}$	310	660	864	290	190	117 μM	Chen et al. (2023)
28	Taxifolin	10.71	305.0656	305.0656	POS	$C_{15}H_{12}O_7$	15,139	1,282,552	13,615	12,993	11,203	125 μM (TAS2R 39)	Roland et al. (2013)
29	Epigallocatechin gallate	1.66	457.0786	457.0776	NEG	$C_{22}H_{18}O_{11}$	344	2684	885	838	174	380 μM	Soares et al. (2018)
30	Caffeic acid	3.58	181.0494	181.0495	POS	$C_9H_8O_4$	15,598,704	67,398,734	8,425,487	8,030,641	7,711,503	538 μM	Shi et al. (2022)
31	Hesperidin	4.09	611.1974	611.1982	POS	$C_{28}H_{34}O_{15}$	234,889	671,215	210,091	200,314	192,029	75 μM	Chen et al. (2023)
32	Vanilic acid hexoside	4.48	329.0874	329.0878	NEG	$C_{14}H_{18}O_9$	2,726,073	4,274,612	921,007	583,690	294,692	–	Banerjee and Preissner (2018a)
33	Petunidin 3-O-(6-acetyl-glucoside)	7.03	522.1375	522.1373	POS	$C_{24}H_{25}O_{13}$	50,460	71,413	67,221	84,213	91,742	–	Banerjee and Preissner (2018a)
34	5-hydroxy-methylfurfural	5.56	127.0391	127.0395	POS	$C_6H_6O_3$	N.D.	N.D.	311,022	1,033,128	2,079,327	30 μM	Li et al. (2021)
35	5-Methylfurfural	15.42	111.1201	111.1201	POS	$C_6H_6O_2$	N.D.	N.D.	14,080	31,830	69,880	4.4 μM	Li et al. (2021)
36	3-Deoxyglucosone	6.07	163.1489	163.1491	POS	$C_6H_{10}O_5$	N.D.	N.D.	41,190	108,410	220,020	*Sweerness (77 %)	Banerjee and Preissner (2018a)
37	2,3-dihydro-3,5-dihydroxy-6-methyl-4(H)-pyran-4-one (DDMP)	5.22	145.0495	145.0488	POS	$C_6H_8O_4$	N.D.	N.D.	23,671	364,487	1,079,327	14.3 μM	Li et al. (2019)
38	Quinizolate	19.01	338.3394	338.339	POS	$C_{19}H_{15}NO_5$	N.D.	N.D.	0	0	646	0.25 μM	Frank et al. (2003)
39	Fructosyl-lysine	4.97	309.1656	309.1656	POS	$C_{12}H_{24}N_2O_7$	N.D.	N.D.	229,024	663,117	815,454	*Bitterness (68.8 %)	Banerjee and Preissner (2018a)
40	Pyrraline	13.49	253.1183	253.119	NEG	$C_{12}H_{18}N_2O_4$	N.D.	N.D.	0	3110	15,262	*Bitterness (71.2 %)	Banerjee and Preissner (2018a)

"N.D.": Not Detected.
"–": there is no threshold information of the compound.
"*": the sense of taste was predicted by BitterSweetForest.
TAS2R39: TAS2R is bitter taste receptor, and the thresholds were measured by No. 39 receptor of TAS2R.
m/z exp.: the m/z value detected in the research.
m/z cal: the m/z value calculated based on molecular formula and ion mode.

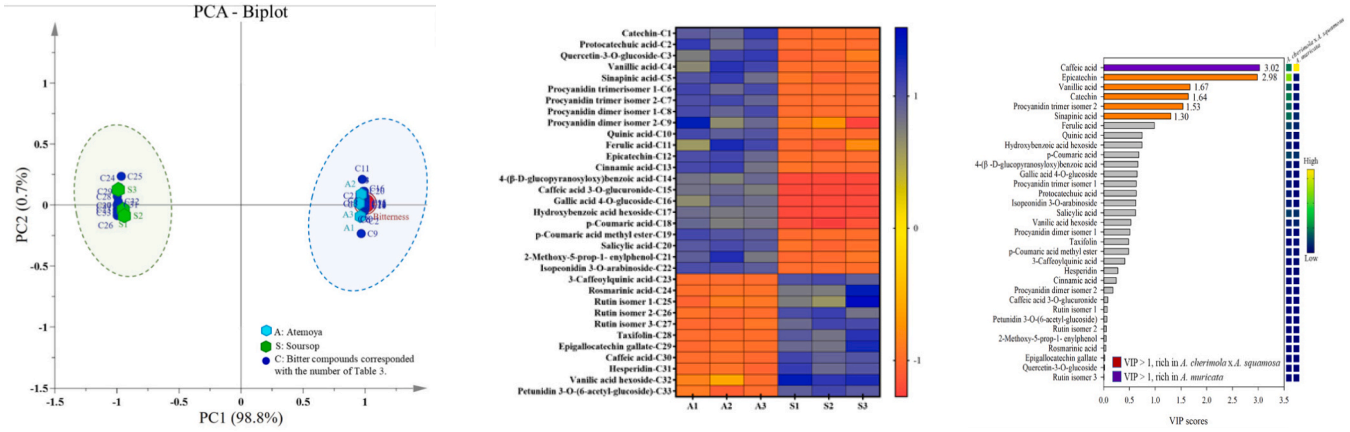

(a) (b) (c)

Fig. 1. (a) PCA-biplot, (b) heat map analysis, and (c) VIP scores (left) and contents (right) of bitter components in *A. cherimola* × *A. squamosa* and *A. muricata*. Data were obtained from LC-HRMS peak area of the compounds in two species. "A", "S" and "C" in PCA-biplot means the variables which were the triplicate of *A. cherimola* × *A. squamosa, A. muricata,* and bitter compounds, respectively. The blue represented high expression, and the red represented low expression in the heat map. The colored mark in VIP scores means VIP > 1, while the orange and the purple of each content represented the compound rich in *A. cherimola* × *A. squamosa* and *A. muricata,* respectively. (For interpretation of the references to color in this figure legend, the reader is referred to the web version of this article.)

of these compounds have been previously reported in various foods and are known to contribute to bitterness. Compounds not referenced in the literature were confirmed for their bitterness using the predictive model–BitterSweetForest (Table 3).

Fig. 2b presents a heat map analysis of the bitterness variables for atemoya and soursop. The peak areas of 33 potential bitter compounds in the two varieties were standardized using Pareto scaling, and the standardized data were visualized in a heat map to illustrate the differences in compound variation between the two varieties. The color gradient of the sample blocks, ranging from red to dark blue, represents the compound content from low to high. The result showed that 11 potential bitter compounds were present at higher levels in soursop, whereas the levels of the other 22 potential bitter compounds were in atemoya. Thus, the potential bitter compounds with higher content in soursop might not predominately lead to the bitterness in atemoya because of the non-bitter characteristic of soursop, and the ones higher in atemoya were speculated as the main reason for the bitterness in atemoya compared with soursop.

OPLS-DA can be used to distinguish and identify sample groups and to find the most important differential variables with strong discriminative ability, serving as indicators for differentiating between samples. By using OPLS-DA, the VIP for each bitter compound variable can be calculated. This allows for the simultaneous assessment of the magnitude of variation between groups and the proportion of total data represented by that variable. Bitter compounds with a VIP value greater than 1 are considered important differential variables, representing the primary differences between the two species and explaining the bitterness differences between them (Galindo-Prieto et al., 2014). In Fig. 1c, six bitter compounds had a VIP value of >1. Although caffeic acid might contribute to the difference between the two species, it was not speculated as the main compound causing the bitterness between the two species because it is rich in soursop. The other five potential bitter compounds were rich in atemoya: epicatechin, vanillic acid, catechin, procyanidin trimer, and sinapic acid. These five identified bitter compounds constituted the major portion of all detected bitter constituents and significantly contributed to the bitterness, suggesting that these compounds are the primary reason atemoya has a more bitter taste than soursop.

3.3. Sensory-guided fractionation of the bitter compounds in atemoya

The results of the sensory evaluation of the compounds (Supplementary Fig. 1.), obtained through sensory guidance and the LC-HRMS analysis of the components, are summarized using PCA and presented in Fig. 2a. The first and second principal components accounted for 50.60 % and 35.50 % of the data variance, respectively, and their sum explained 86.10 % of the total variance, indicating that the principal components effectively fitted with the data (Suhr, 2005). The separation or overlapping between the variables on the PCA biplot represents their correlation. As distances decrease, the strength of the correlation increases. The four fractions were separated from each other in quadrants, indicating the differences between these fractions. On the contrary, F-I-B and F-I-C exhibited a high correlation to bitter intensity. The bitter compound variables in the middle of F-I-B and F-I-C indicated a high correlation to bitter intensity as well, including catechin, epicatechin, quercetin-3-*O*-glucoside, two types of procyanidin dimers, two types of procyanidin trimers, epicatechin gallate, cinnamic acid, caffeoylquinic acid, three types of rutin isomer, taxifolin, epigallocatechin gallate, petunidin-3-*O*-6-acetylglucoside, 4-(*β*-D-glucopyranosyloxy)benzoic acid, vanilic acid hexoside, caffeic acid 3-*O*-glucuronide, gallic acid 4-*O*-glucoside, and 2-Methoxy-5-prop-1-enylphenol, hydroxybenzoic acid hexoside.

The distribution of bitter compounds could be discerned through a heatmap (Fig. 2b). The results indicated 1, 9, 19, and 4 of bitter compounds were the highest in F-I-A, F-I-B, F-I-C, and F-I-D, respectively. The 28 bitter compounds were predominantly distributed in F-I-B and F-I-C, aligning with these two extracts' observed highest bitterness intensity. On the contrary, rosmarinic acid and naringin might predominantly contribute to the weak bitterness in F-I-A, consistent with the hypotheses of Supplementary Fig. 1. Overall, 28 bitter compounds were found in F-I-B and F-I-C. Further confirmation was required through statistical methods to assess the individual contributions of each compound to bitterness. The VIP, representing the significance of bitter compound variables that contributed to bitter intensity, was presented alongside the heat map of the peak area of bitter compounds in Fig. 2c. A total of 10 bitter compounds met the criterion VIP of >1, indicating a strong contribution to the variable of bitter intensity, including catechin, epicatechin, two isomers of procyanidin trimer, two isomers of procyanidin dimers, quinic acid, 4-(*β*-D-glucopyranosyloxy) benzoic acid, hydroxybenzoic acid hexoside, and caffeic acid. Notably, the heatmap

Table 3
Profiling potential bitterness compounds in atemoya to other foods.

Compound No.	Tentative assignment	Cause of bitterness in Other food	Reference
1	Catechin	Wine	Hufnagel and Hofmann (2008)
2	Protocatechuic acid	Beer	Yan and Tong (2023)
3	Quercetin-3-O-glucoside	Hops	Dresel et al. (2015)
4	Vanillic acid	Wine	Hufnagel and Hofmann (2008)
5	Sinapinic acid	Canola Meal	Rubino et al. (1996)
6	Procyanidin trimer isomer 1	Grape seeds	Soares et al. (2018)
7	Procyanidin trimer isomer 2	Grape seeds	Soares et al. (2018)
8	Procyanidin dimer isomer 1	Grape seeds	Soares et al. (2018)
9	Procyanidin dimer isomer 2	Wine	Hufnagel and Hofmann (2008)
10	Quinic acid	Roast coffee	Frank et al. (2006b)
11	Ferulic acid	Beer	Yan and Tong (2023)
12	Epicatechin	Green tea	Chen et al. (2022b)
13	Cinnamic acid	Beer	Yan and Tong (2023)
14	4-(β-D-glucopyranosyloxy) benzoic acid	Machine learning model-BitterSweetForest	Banerjee and Preissner (2018b)
15	Caffeic acid 3-O-glucuronide	Machine learning model-BitterSweetForest	Banerjee and Preissner (2018b)
16	Gallic acid 4-O-glucoside	Machine learning model-BitterSweetForest	Banerjee and Preissner (2018b)
17	Hydroxybenzoic acid hexoside	Machine learning model-BitterSweetForest	Banerjee and Preissner (2018b)
18	p-Coumaric acid	Corn Germ Protein	Huang and Zayas (1991)
19	p-Coumaric acid methyl ester	Hops	Dresel et al. (2015)
20	Salicylic acid	Machine learning model-BitterSweetForest	Banerjee and Preissner (2018b)
21	2-Methoxy-5-prop-1-enylphenol	Machine learning model-BitterSweetForest	Banerjee and Preissner (2018b)
22	Isopeonidin 3-O-arabinoside	Machine learning model-BitterSweetForest	Banerjee and Preissner (2018b)

color gradients for these eight compounds spanned from yellow to green, indicating their predominant presence in the bitter compound content, which suggested that these compounds contribute significantly to the strong bitterness in F-I-B and F-I-C extracts.

In conjunction with Fig. 2d, which utilized the S-plot to illustrate the correlation between latent bitter compound variables and bitter intensity, X-axis imaging shows the magnitude of change (covariance). In contrast, the Y-axis represents the correlation between bitter compound and bitter intensity variables. Eight bitter compounds that met VIP >1 was highly positively correlated with bitter intensity, whereas in others, two bitter compounds exhibited a negative correlation with bitter intensity. Thus, the eight bitter compounds contribute substantially to the bitterness of atemoya. Integrating the results of 3.1 and 3.2, catechin, epicatechin, and procyanidin trimer isomer 2 emerged as significant differential variables, contributing notably to the bitter intensity. These compounds are key to understanding the natural bitterness of atemoya. In the analysis of polyphenolic compounds in atemoya, the primary phenolic compounds identified in the pulp included catechin, epicatechin, procyanidin B1 (procyanidin dimer), procyanidin B2 (procyanidin dimer), and procyanidin C1 (procyanidin trimer). These findings align with the results related to bitter compounds in atemoya (Kumazawa et al., 2007). Previous study have reported, the concentrations of catechin, epicatechin, and procyanidin C1 (procyanidin trimer) in the pulp were 1075, 759, and 662 μM, respectively. Among them, the concentrations of catechin and procyanidin C1 (procyanidin trimer) exceeded their bitter thresholds of 1000 and 400 μM, respectively (Kumazawa et al., 2007), whereas epicatechin only differs from the threshold concentration by pproximately 12 %. The primary bitter compounds in the pulp of atemoya were catechin, epicatechin, and procyanidin trimer.

3.4. Effect of commercial thermal treatment on phytochemicals and 5-HMF in atemoya

Table 4 shows that the phytochemical content of commercially sterilized atemoya is relatively higher than that of untreated atemoya. It shows that thermal processing causes the covalent bonds of bound phenols in the original cell wall structure to be broken and released, making the phytochemicals in atemoya easier to detect.

The decline of flavonoids in AP-85 may be attributed to their primary mode of binding to cell wall matrix, such as pectin and cellulose, which involves the dehydration of hydroxyl groups to form glycosidic linkages. In a low-pH pulp environment, compared with the use of carboxyl groups to form phenolic acids with ether bonds and glycosidic bonds of flavonoids are more easily hydrolyzed in acidic environments (Acosta-Estrada et al., 2014). The pH of atemoya pulp is about 4.56 (Orsi et al., 2012). In addition, we speculated that the thermal treatment of AP-75 can fully release the flavonoids bound to the pulp. The increase in AP-85 increases the degradation rate of flavonoids, resulting in a downward trend in the total flavonoid content (Chaaban et al., 2017).

Based on the above results, the increase in total phytochemical content caused by thermal processing may lead to an increase in bitter substances. However, depending on the structure of the compound and the composition of the bound phytochemicals, the trend of increasing and decreasing the content during thermal processing is also different, so further identification is still needed to confirm the key compounds responsible for the bitter taste.

Table 4 shows that in the untreated group, AP-65, AP-75, and AP-85, the glucose contents were 188.89 ± 11.49, 167.30 ± 8.24, 152.39 ± 8.13, 141.09 ± 8.01 mg/g, and 209.11 ± 9.34 mg/g, respectively. The fructose contents were 166.81 ± 8.44, 130.96 ± 7.99, and 114.24 ± 7.99 mg/g, respectively.

In the untreated group, AP-65, AP-75, and AP-85, the 5-HMF contents were 147.16 ± 3.32, 400.71 ± 3.08, 1208.59 ± 8.12, 2838.51 ± 13.02 ng/g, respectively. With the increase of thermal processing intensity, the 5-HMF increases significantly, indicating that in these three thermal treatment groups, the Maillard reaction is mainly in the middle stage of the reaction (Gao et al., 2019).

The sensory bitterness threshold of 5-HMF in water is 3780 ng/g (Li et al., 2021). The AP-85 treatment group with the highest 5-HMF content contained 2838.51 ± 13.02 ng/g, lower than the lowest threshold for 5-HMF to trigger bitterness. Therefore, this result triggers speculation that the Maillard reaction did not contribute to the bitterness of the three thermal processing groups.

3.5. Metabolomic analysis of the effects of thermal treatment on compounds in atemoya

Table 2 shows that a total of 39 bitter components were found in the 95 % ethanol extracts of the untreated group, AP-65, AP-75, and AP-85, of which 33 were the natural bitter compounds of atemoya found in

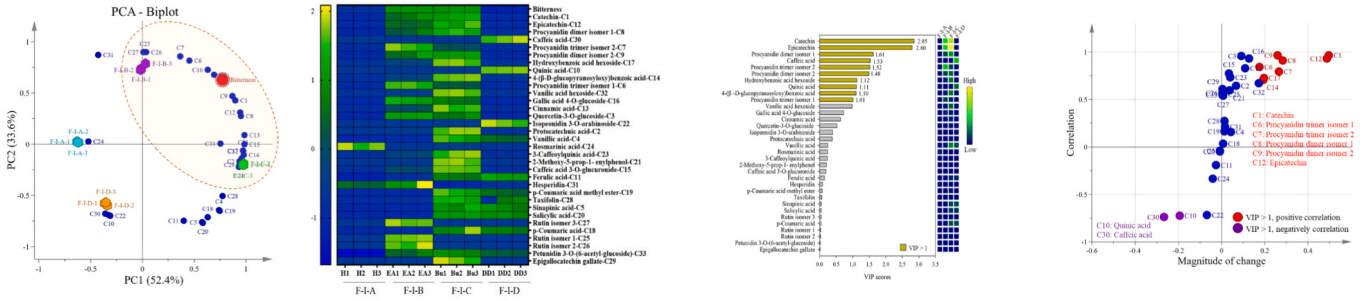

(a) (b) (c) (d)

Fig. 2. (a) PCA-biplot of bitter components, (b) heat map analysis of bitter components, (c) VIP scores (left) and contents (right), and (d) S-Plot of the bitter components from OPLS model in the sensory-guided extracts of freeze-dried *A. cherimola* × *A. squamosa*. Data were obtained from LC-HRMS peak area and sensory bitter intensities of the sensory-guided extracts of freeze-dried *A. cherimola* × *A. squamosa*. The green represents high expression and the blue represents low expression in heat map. Colored mark in VIP scores means VIP > 1. (For interpretation of the references to color in this figure legend, the reader is referred to the web version of this article.)

Table 4
Glucose, fructose, 5-HMF, Total phenolics, total flavonoids, and total tannins of untreated and thermally treated (AP-65, AP-75, and AP-85) *A. cherimola* × *A. squamosa* samples.

Parameter	Untreated	AP-65	AP-75	AP-85
Glucose (mg/g)	188.89 ± 11.49^{a}	167.30 ± 8.24^{b}	152.39 ± 8.13^{c}	141.09 ± 8.01^{d}
Fructose (mg/g)	209.11 ± 9.34^{a}	166.81 ± 8.44^{b}	130.96 ± 7.99^{c}	114.24 ± 7.99^{d}
5-HMF (ng/g)	23.16 ± 3.32^{d}	400.71 ± 3.08^{c}	1208.59 ± 8.12^{b}	2838.51 ± 13.02^{a}
Phenolics (mg/g)	3.76 ± 0.20^{d}	4.25 ± 0.23^{c}	4.63 ± 0.25^{b}	4.82 ± 0.24^{a}
Flavonoids (mg/g)	0.40 ± 0.01^{d}	0.58 ± 0.06^{c}	0.87 ± 0.08^{a}	0.77 ± 0.05^{b}
Tannins (mg/g)	2.74 ± 0.13^{c}	2.85 ± 0.01^{c}	3.15 ± 0.07^{b}	3.33 ± 0.07^{a}

Data are represented as means ± standard deviations for three replicates. Different letters show significant differences ($p < 0.05$) in the same measurement among treatments.

Table 2, and the rest were 6 species are the mid-stage maillard reaction products in the thermal processing group (Gao et al., 2019).

Fig. 3a and b are principal component dual sequence diagrams and heat maps obtained by bringing in the peak areas and sensory evaluation results of 39 bitter compounds from the untreated and three thermal treatment groups. The first and second principal component axes of the principal component bisequence plot can explain 67.3 % and 18.4 % of the data variability, respectively, and can explain 86.10 % of the total data variability.

Fig. 3a, the variable points of the four treatment groups are distributed in the four quadrants of the principal component bisequence diagram, indicating that with higher temperatures, the composition of the treatment groups changes and differs. A shorter distance between the compound variable and a given treatment group variable indicates a stronger correlation between the compound variable and the treatment group. It also suggests that the compound variable is more prevalent in the treatment group. There are 15 compound variables adjacent to the variable point of the untreated group, indicating that its content is the highest in the untreated group, and thermal processing may cause degradation and reduce the content.

There are 5 compound variables adjacent to the AP-65 group variables. Fig. 3b shows that these 5 compounds all have the highest content in AP-65 and decrease in order among AP-75 and AP-85. This finding shows that thermal processing may promote the release of bound phytochemicals and cause the compound content to increase in AP-65, but it increases with the temperature. The thermal degradation of the compounds was aggravated, causing their contents in AP-75 and AP-85 to drop to close to or lower than those in the untreated group. Therefore, we speculate that the compounds are not the main contributor to the heated bitterness.

There are 5 compound variables adjacent to the AP-75 group variable. The combined heat map shows that these 5 compounds all have an increasing trend from AP-65 to AP-75. The highest content was present

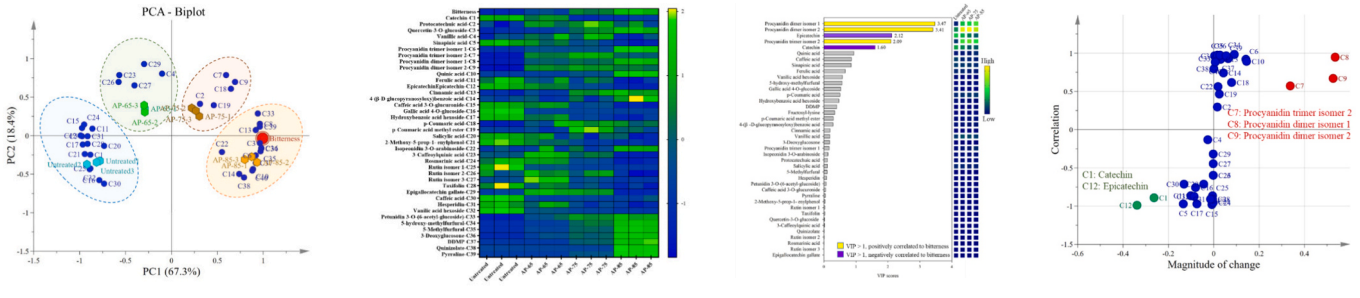

(a) (b) (c) (d)

Fig. 3. (a) PCA-biplot of bitter components, (b) heat map analysis of bitter components, (c) VIP scores (left) and contents (right), and (d) S-Plot of the bitter components from OPLS model in untreated and thermal treatments (AP-65, AP-75, and AP-85) of *A. cherimola* × *A. squamosa*. Data were obtained from LC-HRMS peak area and bitter intensities of each treatment *A. cherimola* × *A. squamosa*. The green represents high expression, and the blue represents low expression in a heat map. Color mark in VIP scores means VIP > 1. (For interpretation of the references to color in this figure legend, the reader is referred to the web version of this article.)

in AP-75 and decreased in the AP-85 group. However, these bitter compounds still showed a higher content in AP-85 compared to the untreated group, partially contributing to the bitter taste of thermal processing. There are 14 compound variables adjacent to the AP-85 group variables.

When analyzed alongside the heat map, it becomes evident that the concentrations of these 14 compounds rise with increasing thermal treatment temperatures, reaching their peak levels in the AP-85 group. This result raises speculation that these bitter compounds contribute to the bitter taste of thermal processing. The results of the combined principal component bisequence map and heat map showed that a total of 19 bitter compounds contributed to the bitterness of thermal processing of atemoya, namely protocatechuic acid, quercetin-3-O-glucoside, vanillic acid, procyanidin trimer isomer 1 & 2, procyanidin dimer isomer 1 & 2, quinic acid, cinnamic acid, 4-(β-D-glucopyranosyloxy)benzoic acid, p-coumaric acid, p-coumaric acid methyl ester, isopeonidin 3-O-arabinoside and petunidin 3-O-(6-acetyl-glucoside). Most of these compounds have been previously reported in various foods and are known to contribute to bitterness. Compounds not referenced in the literature were confirmed for their bitterness using the predictive model–BitterSweetForest (Table 3).

Fig. 3c shows that there are 5 bitter chemicals with VIP > 1, which are substantially linked with the bitterness intensity variable and are considered relevant differential factors. They are 2 proanthocyanidin dimers and proanthocyanidin trimer isomers 1, Catechins and catechins. When combined with Fig. 3b, it can be found that the peak areas of 5 compounds with VIP values greater than 1 account for the main proportion among the 39 bitter compounds. Among them, epicatechin and catechin are the most abundant bitter substances in the unprocessed pulp of atemoya. However, it continues to decrease with the increase in thermal processing intensity. Fig. 3d demonstrates a negative correlation with the trend of bitterness intensity. This pattern may be attributed to the accelerated degradation of flavonoids in the acidic environment of atemoya pulp during thermal processing (Moussa-Ayoub et al., 2011).

3.6. Speculation on the cause of the bitter taste of atemoya caused by thermal processing

As shown in Fig. 4a, the mean degree of polymerization (mDP) of proanthocyanidins in the untreated group, AP-65, AP-75, and AP-85 were 3.38 ± 0.25, 2.92 ± 0.16, 2.70 ± 0.11, and 2.55 ± 0.06, respectively. The mDP of the thermal processing group showed a significant decrease compared with the untreated group and decreased with the heating temperature in a dose-effect manner (Salazar-Orbea et al., 2023). When the degree of proanthocyanin is higher, the astringent taste is mainly present. As the degree of polymerization decreases, the astringency gradually decreases, and the bitterness increases. Proanthocyanidins with a polymerization degree of 6–8 or higher primarily exhibit an astringent taste, while those with a lower degree tend to have a bitter taste. The reason why proanthocyanidin dimers and trimers increase significantly after thermal processing is the release of bound phytochemicals (Shahidi & Yeo, 2016). The results are consistent with sensory evaluation (Supplementary Fig. 2), showing that the bitter intensity of atemoya increases with extended heating time.

The thermal processing process not only causes the degree of proanthocyanin to decrease but also the flavonoids produced during the cracking process of proanthocyanin will also be oxidized (low pH value) into proanthocyanidin aglycones that can combine with sugar to form proanthocyanidins (El Rayess et al., 2014). Proanthocyanidin aglycones can also form dimer proanthocyanidins with catechin and epicatechin, and the continued degradation of proanthocyanidins will also accumulate low-polymerization proanthocyanidins such as dimers and trimers (Haslam et al., 1988; Luo et al., 2018).

The pH value of atemoya is 4.5, and the degree of proanthocyanidin aglycones will decrease during thermal processing (Fig. 4a). From Table 4, we can also find an increase in flavonoids and a decrease in sugars, which may indicate that atemoya undergoes thermal processing. The bitter taste during processing is caused by the increase in the total amount of proanthocyanidins, the decrease in the polymerization degree of proanthocyanidins, and the accumulation of low-polymerization proanthocyanidins (Fig. 4b).

This carbocation is highly reactive and can be oxidized under acidic conditions. It is proanthocyanidins aglycone and combines with sugar to form proanthocyanidins. Depending on the form and quantity of proanthocyanidins bonding with sugar molecules, it may cause the bitter taste of food (El Rayess et al., 2014).

Alternatively, it can form a dimer of proanthocyanidins with catechin and epicatechin. The degradation of proanthocyanidins will also cause the accumulation of dimers, trimers, and other low-polymerization proanthocyanidins (Haslam et al., 1988; Luo et al., 2018) (Fig. 4b). All three mechanisms may lead to the increase of bitter substances, resulting in the bitter taste of atemoya due to thermal processing.

4. Conclusion

In this study, the combination of sensory-guided separation with OPLS-PCA analysis and LC-HRMS identified that catechins, epicatechins, and proanthocyanidin trimers compound native to atemoya and absent in soursop is the cause of the distinct bitter taste in atemoya

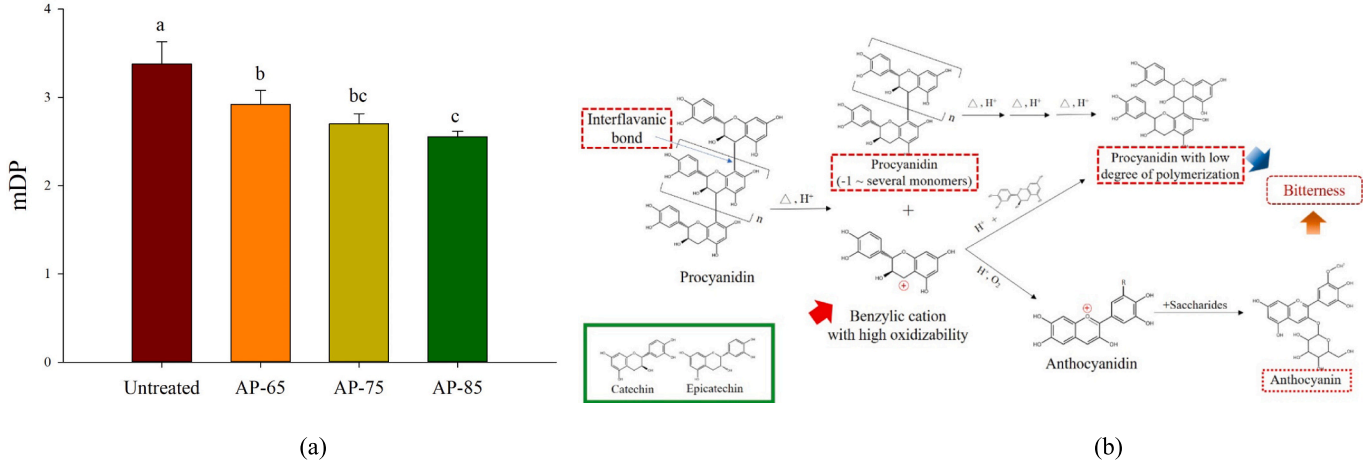

Fig. 4. (a) Effect of thermal processing on the mDP of proanthocyanidins in *A. cherimola* × *A. squamosa*. (b) Potential mechanisms of the transformation of procyanidins led by thermal processing.

following freeze-drying. Further analysis, employing several thermal treatment temperatures and LC-HRMS, revealed that atemoya generates 5-HMF via the Maillard reaction during thermal processing. However, the concentration of 5-HMF remains below the bitterness threshold and correlates with the bitter taste profile identified in OPLS-PCA analysis. In addition, this study discovered that the degradation of proanthocyanidin dimers and trimers affects atemoya puree during thermal processing, based on an OPLS-PCA thorough analysis of LC-HRMS and sensory guidance and taste assessment results. Moreover, the results of this study further reveal that the factors affecting the flavor of the thermal processing of fruits may not entirely come from Maillard reaction products but may more likely come from the structural transformation of phytochemicals.

Ethical statement

Ethical approval for the involvement of human subjects in this study was granted by National Cheng Kung University Medical College-Human Research Ethics Review Committee, Reference number B-ER-111-438. Participants gave informed consent via the statement "I am aware that my responses are confidential, and I agree to participate in this survey" where an affirmative reply was required to enter the survey. They were able to withdraw from the survey at any time without giving a reason. The products tested were safe for consumption. The study was explained to consumers in the questionnaire, that all data will be de-identified and only reported in the aggregate. All participants acknowledged an informed consent statement in order to participate in the study.

CRediT authorship contribution statement

Erh-Kang Luo: Writing – review & editing, Writing – original draft, Visualization, Investigation, Data curation, Conceptualization. **Chun-Ting Lin:** Writing – review & editing, Writing – original draft, Visualization, Software, Methodology, Investigation, Data curation, Conceptualization. **Chao-Kai Chang:** Writing – review & editing, Writing – original draft, Visualization, Software, Methodology, Data curation, Conceptualization. **Nai-Wen Tsao:** Software, Methodology, Conceptualization. **Chih-Yao Hou:** Visualization, Validation, Software, Investigation. **Min-Hung Chen:** Supervision. **Sheng-Yen Tsai:** Writing – review & editing, Writing – original draft, Software, Methodology, Conceptualization. **Chang-Wei Hsieh:** Writing – review & editing, Validation, Software, Methodology, Conceptualization.

Declaration of competing interest

None.

Data availability

Data will be made available on request.

Acknowledgments

This work was financially supported (in part) by the Advanced Plant and Food Crop Biotechnology Center from The Featured Areas Research Center Program within the framework of the Higher Education Sprout Project by the Ministry of Education (MOE) and National Science and Technology Council (NSTC 112-2320-B-005-004-MY3) in Taiwan.

Appendix A. Supplementary data

Supplementary data to this article can be found online at https://doi.org/10.1016/j.fochx.2024.101817.

References

Acosta-Estrada, B. A., Gutiérrez-Uribe, J. A., & Serna-Saldívar, S. O. (2014). Bound phenolics in foods, a review. *Food Chemistry, 152*, 46–55.

Banerjee, P., & Preissner, R. (2018a). BitterSweetForest: A random forest based binary classifier to predict bitterness and sweetness of chemical compounds. *Frontiers in Chemistry, 6*, 93.

Banerjee, P., & Preissner, R. (2018b). BitterSweetForest: A random Forest based binary classifier to predict bitterness and sweetness of chemical compounds [original research]. *Frontiers in Chemistry, 6*. https://doi.org/10.3389/fchem.2018.00093

Baskaran, R., Ravi, R., & Rajarathnam, S. (2016). Thermal processing alters the chemical quality and sensory characteristics of sweetsop (*Annona squamosa* L.) and soursop (*Annona muricata* L.) pulp and nectar. *Journal of Food Science, 81*(1), S182–S188. https://doi.org/10.1111/1750-3841.13165

Bin, Q., & Peterson, D. G. (2016). Identification of bitter compounds in whole wheat bread crumb. *Food Chemistry, 203*, 8–15. https://doi.org/10.1016/j.foodchem.2016.01.116

Capuano, E., & Fogliano, V. (2011). Acrylamide and 5-hydroxymethylfurfural (HMF): A review on metabolism, toxicity, occurrence in food and mitigation strategies. *LWT-Food Science and Technology, 44*(4), 793–810.

Chaaban, H., Ioannou, I., Chebil, L., Slimane, M., Gérardin, C., Paris, C., … Ghoul, M. (2017). Effect of heat processing on thermal stability and antioxidant activity of six flavonoids. *Journal of Food Processing and Preservation, 41*(5), Article e13203.

Chang, C.-K., Yang, Y.-T., Gavahian, M., Cheng, K.-C., Hou, C.-Y., Chen, M.-H., … Hsieh, C.-W. (2023). Prolonging the shelf-life of atemoya (*Annona cherimola* × *Annona squamosa*) using pulsed electric field treatments. *Innovative Food Science & Emerging Technologies, 88*. https://doi.org/10.1016/j.ifset.2023.103458

Chen, F., Du, X., Zu, Y., Yang, L., & Wang, F. (2016). Microwave-assisted method for distillation and dual extraction in obtaining essential oil, proanthocyanidins and polysaccharides by one-pot process from Cinnamomi cortex. *Separation and Purification Technology, 164*, 1–11.

Chen, L., Lin, Y., Yan, X., Ni, H., Chen, F., & He, F. (2023). 3D-QSAR studies on the structure–bitterness analysis of citrus flavonoids. *Food & Function, 14*(10), 4921–4930.

Chen, Y.-H., Zhang, Y.-H., Chen, G.-S., Yin, J.-F., Chen, J.-X., Wang, F., & Xu, Y.-Q. (2022a). Effects of phenolic acids and quercetin-3-O-rutinoside on the bitterness and astringency of green tea infusion. *npj Science of Food, 6*(1), 1–8.

Chen, Y.-H., Zhang, Y.-H., Chen, G.-S., Yin, J.-F., Chen, J.-X., Wang, F., & Xu, Y.-Q. (2022b). Effects of phenolic acids and quercetin-3-O-rutinoside on the bitterness and astringency of green tea infusion. *npj Science of Food, 6*(1), 8. https://doi.org/10.1038/s41538-022-00124-8

Degenhardt, A. G., & Hofmann, T. (2010). Bitter-tasting and Kokumi-enhancing molecules in thermally processed avocado (*Persea americana* Mill.). *Journal of Agricultural and Food Chemistry, 58*(24), 12906–12915. https://doi.org/10.1021/jf103848p

Dresel, M., Dunkel, A., & Hofmann, T. (2015). Sensomics analysis of key bitter compounds in the hard resin of hops (*Humulus lupulus* L.) and their contribution to the bitter profile of pilsner-type beer. *Journal of Agricultural and Food Chemistry, 63*(13), 3402–3418. https://doi.org/10.1021/acs.jafc.5b00239

El Rayess, Y., Barbar, R., Wilson, E. A., & Bouajila, J. (2014). *Analytical methods for wine polyphenols analysis and for their antioxidant activity evaluation* (pp. 71–101). New York, NY, USA: Nova Science Publishers.

Elmas, F., Varhan, E., & Koç, M. (2019). Drying characteristics of jujube (*Zizyphus jujuba*) slices in a hot air dryer and physicochemical properties of jujube powder. *Journal of Food Measurement and Characterization, 13*, 70–86.

Feumba Dibanda, R., Panyoo Akdowa, E., Rani, P. A., Metsatedem Tongwa, Q., & Mbofung, F. C. M. (2020). Effect of microwave blanching on antioxidant activity, phenolic compounds and browning behaviour of some fruit peelings. *Food Chemistry, 302*, Article 125308. https://doi.org/10.1016/j.foodchem.2019.125308

Frank, O., Jezussek, M., & Hofmann, T. (2003). Sensory activity, chemical structure, and synthesis of Maillard generated bitter-tasting 1-oxo-2, 3-dihydro-1 H-indolizinium-6-olates. *Journal of Agricultural and Food Chemistry, 51*(9), 2693–2699.

Frank, O., Zehentbauer, G., & Hofmann, T. (2006a). Bioresponse-guided decomposition of roast coffee beverage and identification of key bitter taste compounds. *European Food Research and Technology, 222*, 492–508.

Frank, O., Zehentbauer, G., & Hofmann, T. (2006b). Bioresponse-guided decomposition of roast coffee beverage and identification of key bitter taste compounds. *European Food Research and Technology, 222*(5), 492–508. https://doi.org/10.1007/s00217-005-0143-6

Galindo-Prieto, B., Eriksson, L., & Trygg, J. (2014). Variable influence on projection (VIP) for orthogonal projections to latent structures (OPLS). *Journal of Chemometrics, 28*(8), 623–632.

Gao, C., Tello, E., & Peterson, D. G. (2021). Identification of coffee compounds that suppress bitterness of brew. *Food Chemistry, 350*, Article 129225. https://doi.org/10.1016/j.foodchem.2021.129225

Gao, C., Tello, E., & Peterson, D. G. (2023). Identification of compounds that enhance bitterness of coffee brew. *Food Chemistry, 415*, Article 135674. https://doi.org/10.1016/j.foodchem.2023.135674

Gao, Q., Jiang, H., Tang, F., Cao, H. Q., Wu, X. W., Qi, F. F., … Yang, J. (2019). Evaluation of the bitter components of bamboo shoots using a metabolomics approach. *Food & Function, 10*(1), 90–98. https://doi.org/10.1039/c8fo01820k

García, J. M., Prieto, L. J., Guevara, A., Malagon, D., & Osorio, C. (2016). Chemical studies of yellow tamarillo (*Solanum betaceum* Cav.) fruit flavor by using a molecular sensory approach. *Molecules, 21*(12), 1729.

Gökmen, V., Açar, Ö.Ç., Köksel, H., & Acar, J. (2007). Effects of dough formula and baking conditions on acrylamide and hydroxymethylfurfural formation in cookies. *Food Chemistry, 104*(3), 1136–1142.
Habschied, K., Košir, I. J., Krstanović, V., Kumrić, G., & Mastanjević, K. (2021). Beer polyphenols—Bitterness, astringency, and off-flavors. *Beverages, 7*(2), 38.
Haslam, E., Lilley, T. H., & Butler, L. G. (1988). Natural astringency in foodstuffs—A molecular interpretation. *Critical Reviews in Food Science and Nutrition, 27*(1), 1–40.
Huang, C., & Zayas, J. (1991). Phenolic acid contributions to taste characteristics of corn germ protein flour products. *Journal of Food Science, 56*(5), 1308–1310.
Hufnagel, J. C., & Hofmann, T. (2008). Orosensory-directed identification of astringent mouthfeel and bitter-tasting compounds in red wine. *Journal of Agricultural and Food Chemistry, 56*(4), 1376–1386. https://doi.org/10.1021/jf073031n
Kalalinia, F., Amiri, N., Mehrvarzian, N., Bazzaz, B. S. F., Iranshahi, M., Shahroodi, A., … Movaffagh, J. (2020). Topical green tea formulation with anti-hemorrhagic and antibacterial effects. *Iranian Journal of Basic Medical Sciences, 23*(6). https://doi.org/10.22038/ijbms.2020.41397.9782
Kumazawa, S., Ikenaga, M., Usui, Y., Kajiya, K., Miwa, S., Endo, J., … Nakayama, T. (2007). Comprehensive analysis of polyphenols in fruits consumed in Japan. *Food Science and Technology Research, 13*(4), 404–413. https://doi.org/10.3136/fstr.13.404
Li, H., Tang, X., Wu, C., & Yu, S. (2019). Formation of 2, 3-dihydro-3, 5-Dihydroxy-6-Methyl-4 (H)-Pyran-4-one (DDMP) in glucose-amino acids Maillard reaction by dry-heating in comparison to wet-heating. *LWT, 105*, 156–163.
Li, H., Zhang, W. C., Tang, X. Y., Wu, C. J., Yu, S. J., & Zhao, Z. Q. (2021). Identification of bitter-taste compounds in class-III caramel colours. *Flavour and Fragrance Journal, 36*(3), 404–411.
Li, M., Chen, X., Deng, J., Ouyang, D., Wang, D., Liang, Y., Chen, Y., & Sun, Y. (2020). Effect of thermal processing on free and bound phenolic compounds and antioxidant activities of hawthorn. *Food Chemistry, 332*, Article 127429.
Liu, F., Chang, X., Hu, X., Brennan, C. S., & Guo, X. (2017). Effect of thermal processing on phenolic profiles and antioxidant activities in *Castanea mollissima*. *International Journal of Food Science & Technology, 52*(2), 439–447.
Luo, L., Cui, Y., Cheng, J., Fang, B., Wei, Z., & Sun, B. (2018). An approach for degradation of grape seed and skin proanthocyanidin polymers into oligomers by sulphurous acid. *Food Chemistry, 256*, 203–211.
Civille, G. V., & Carr, B. T. (2015). *Sensory evaluation techniques*. CRC Press.
de Moraes, M. R., da Silveira, T. F. F., Coutinho, J. P., Souza, D. S., Duarte, M. C. T., Duarte, R. T., … Godoy, H. T. (2021). Bioactivity of atemoya fruits and by-products. *Food Bioscience, 41*, Article 101036. https://doi.org/10.1016/j.fbio.2021.101036
Moraes, M. R.d., Silveira, T. F. F.d., Coutinho, J. P., Souza, D. S., Duarte, M. C. T., Duarte, R. T., … Godoy, H. T. (2021). Bioactivity of atemoya fruits and by-products. *Food Bioscience, 41*. https://doi.org/10.1016/j.fbio.2021.101036
Moussa-Ayoub, T. E., El-Samahy, S. K., Kroh, L. W., & Rohn, S. (2011). Identification and quantification of flavonol aglycons in cactus pear (Opuntia ficus indica) fruit using a commercial pectinase and cellulase preparation. *Food Chemistry, 124*(3), 1177–1184.
Ng, Z. X., & Tan, W. C. (2017). Impact of optimised cooking on the antioxidant activity in edible mushrooms. *Journal of Food Science and Technology, 54*(12), 4100–4111. https://doi.org/10.1007/s13197-017-2885-0
Niwa, T. (1999). 3-Deoxyglucosone: Metabolism, analysis, biological activity, and clinical implication. *Journal of Chromatography B: Biomedical Sciences and Applications, 731*(1), 23–36.
Orsi, D. C., Carvalho, V. S., Nishi, A. C. F., Damiani, C., & Asquieri, E. R. (2012). Use of sugar apple, atemoya and soursop for technological development of jams: Chemical and sensorial composition. *Ciência e agrotecnologia, 36*, 560–566.
Pu, Y., Ding, T., Zhang, N., Jiang, P., & Liu, D. (2017). Identification of bitter compounds from dried fruit of Ziziphus jujuba cv. Junzao. *International Journal of Food Properties, 20*(sup1), S26–S35. https://doi.org/10.1080/10942912.2017.1288133
Qin, D., Wang, Q., Li, H., Jiang, X., Fang, K., Wang, Q., Li, B., Pan, C., & Wu, H. (2020). Identification of key metabolites based on non-targeted metabolomics and chemometrics analyses provides insights into bitterness in Kucha [Camellia kucha (Chang et Wang) Chang]. *Journal of Food Research International, 138*(109789), 8. https://doi.org/10.1016/j.foodres.2020.109789
Ren, Y.-Y., Sun, P.-P., Wang, X.-X., & Zhu, Z.-Y. (2020). Degradation of cell wall polysaccharides and change of related enzyme activities with fruit softening in *Annona squamosa* during storage. *Postharvest Biology and Technology, 166*. https://doi.org/10.1016/j.postharvbio.2020.111203
Roland, W. S., van Buren, L., Gruppen, H., Driesse, M., Gouka, R. J., Smit, G., & Vincken, J.-P. (2013). Bitter taste receptor activation by flavonoids and isoflavonoids: Modeled structural requirements for activation of hTAS2R14 and hTAS2R39. *Journal of Agricultural and Food Chemistry, 61*(44), 10454–10466.
Rubino, M. I., Arntfield, S. D., & Charlton, J. L. (1996). Evaluation of alkaline conversion of sinapic acid to thomasidioic acid. *Journal of Agricultural and Food Chemistry, 44*(6), 1399–1402.
Salazar-Orbea, G. L., García-Villalba, R., Bernal, M. J., Hernández, A., Tomás-Barberán, F. A., & Sánchez-Siles, L. M. (2023). Stability of phenolic compounds in apple and strawberry: Effect of different processing techniques in industrial set up. *Food Chemistry, 401*, Article 134099.
Shahidi, F., & Yeo, J. (2016). Insoluble-bound phenolics in food. *Molecules, 21*(9), 1216.
Shi, Y., Zhang, S., Sun, K., Wang, X., Jiang, J., & Zeng, L. (2022). Characterization of bitter taste theacrine in Pu-erh tea. *Journal of Food Composition and Analysis, 106*, Article 104331.
Shiratake, K., & Martinoia, E. (2007). Transporters in fruit vacuoles. *Plant Biotechnology, 24*(1), 127–133. https://doi.org/10.5511/plantbiotechnology.24.127
Silva, H.d. N., Rabelo, S. V., Diniz, T. C., Oliveira, F. G.d. S., Teles, R. B.d. A., Silva, J. C., … Almeida, J. R. G.d. S. (2017). Antinociceptive and anti-inflammatory activities of ethanolic extract from atemoya (*Annona cherimola* Mill x *Annona squamosa* L.). *African Journal of Pharmacy and Pharmacology, 11*(18), 224–232. https://doi.org/10.5897/ajpp2017.4778
Singh, B. P., & Vij, S. (2018). α-Galactosidase activity and oligosaccharides reduction pattern of indigenous lactobacilli during fermentation of soy milk. *Food Bioscience, 22*, 32–37.
Soares, S., Silva, M. S., García-Estevez, I., Groβmann, P., Brás, N., Brandão, E., … Meyerhof, W. (2018). Human bitter taste receptors are activated by different classes of polyphenols. *Journal of Agricultural and Food Chemistry, 66*(33), 8814–8823. https://doi.org/10.1021/acs.jafc.8b03569
Suhr, D. D. (2005). Principal component analysis vs. exploratory factor analysis. *SUGI 30 proceedings, 203*(30), 10.
Sun, L., Zhang, S., Li, Q., Yuan, E., Chen, R., Yan, F., … Li, Q. (2023). Metabolomics and electronic tongue reveal the effects of different storage years on metabolites and taste quality of Oolong tea. *Food Control, 152*, Article 109847.
Wei, M., Tang, M., Wang, L., Cheng, X., Wu, Y., & Ouyang, J. (2021). Endogenous bioactive compounds of naked oats (*Avena nuda* L.) inhibit α-amylase and α-glucosidase activity. *Lwt, 149*. https://doi.org/10.1016/j.lwt.2021.111902
Wu, C.-T., Huang, W.-H., Dy, K. B., Chang, C.-C., & Hsu, S.-H. (2022). Contribution of active controlled atmosphere (CA) technology to the value-chain of perishable fruits and to rural development: Case of Atemoya in Taiwan. *Sustainability, 14*(23).
Xiang, X., Yang, Q., Chen, K., Wang, Z., Yang, G., Li, A., An, X., & Kan, J. (2024). Characterization of key bitter compounds in Idesia polycarpa var. vestita Diels fruit by sensory-guided fractionation. *Food Chemistry, 439*, Article 138103. https://doi.org/10.1016/j.foodchem.2023.138103
Yan, J., & Tong, H. (2023). An overview of bitter compounds in foodstuffs: Classifications, evaluation methods for sensory contribution, separation and identification techniques, and mechanism of bitter taste transduction. *Comprehensive Reviews in Food Science and Food Safety, 22*(1), 187–232. https://doi.org/10.1111/1541-4337.13067
Yang, Q., Mei, X., Wang, Z., Chen, X., Zhang, R., Chen, Q., & Kan, J. (2021). Comprehensive identification of non-volatile bitter-tasting compounds in Zanthoxylum bungeanum maxim. By untargeted metabolomics combined with sensory-guided fractionation technique. *Food Chemistry, 347*(129085), 11. https://doi.org/10.1016/j.foodchem.2021.129085
Yang, Q., Wang, Z., Chen, X., Guo, Z., Wen, L., & Kan, J. (2022). Evaluation of bitter compounds in Zanthoxylum schinifolium Sieb. Et Zucc. By instrumental and sensory analyses. *Food Chemistry, 390*, Article 133180. https://doi.org/10.1016/j.foodchem.2022.133180